Evaluation of a surrogate contact model in force-dependent kinematic simulations of total knee replacement

Marra, Marco A.; Andersen, Michael S.; Damsgaard, Michael; Koopman, Bart (H.F.J.M); Janssen, Dennis; Verdonschot, Nico

Published in:
Journal of Biomechanical Engineering

DOI (link to publication from Publisher):
10.1115/1.4036605

Publication date:
2017

Document Version
Accepted author manuscript, peer reviewed version

Evaluation of a Surrogate Contact Model in Force-Dependent Kinematic Simulations of Total Knee Replacement

Marco A. Marra[1]
Radboud University Medical Center, Radboud Institute for Health Sciences, Orthopaedic Research Laboratory
P.O.Box 9101, 6500 HB Nijmegen, The Netherlands
Marco.Marra@radboudumc.nl

Michael S. Andersen
Aalborg University, Department of Mechanical and Manufacturing Engineering
Fibigerstraede 16, DK-9220 Aalborg, Denmark
msa@m-tech.aau.dk

Michael Damsgaard
AnyBody Technology A/S
Niels Jernes Vej 10, DK-9220 Aalborg, Denmark
md@anybodytech.com

Bart F.J.M. Koopman
University of Twente, Department of Biomechanical Engineering
P.O.Box 217, 7500 AE Enschede, The Netherlands
h.f.j.m.koopman@utwente.nl

Dennis Janssen
Radboud University Medical Center, Radboud Institute for Health Sciences, Orthopaedic Research Laboratory
P.O.Box 9101, 6500 HB Nijmegen, The Netherlands
Dennis.Janssen@radboudumc.nl

Nico Verdonschot
Radboud University Medical Center, Radboud Institute for Health Sciences, Orthopaedic Research Laboratory
P.O.Box 9101, 6500 HB Nijmegen, The Netherlands
University of Twente, Department of Biomechanical Engineering
P.O.Box 217, 7500 AE Enschede, The Netherlands

[1] Corresponding author
Mailing address: P.O.Box 9101, 6500 HB Nijmegen, The Netherlands
Telephone: +31 (0)24 361 73 79
e-mail: Marco.Marra@radboudumc.nl

38 Nico.Verdonschot@radboudumc.nl

ABSTRACT

Knowing the forces in the human body is of great clinical interest and musculoskeletal models are the most commonly used tool to estimate them in vivo*. Unfortunately, the process of computing muscle, joint contact and ligament forces simultaneously is computationally highly demanding. The goal of this study was to develop a fast surrogate model of the tibiofemoral (TF) contact in a total knee replacement (TKR) model and apply it to force-dependent kinematic simulations of activities of daily living (ADLs). Multiple domains were populated with sample points from the reference TKR contact model, based on reference simulations and design-of-experiments. Artificial neural networks learned the relationship between TF pose and loads from the medial and lateral sides of the TKR implant. Normal and right-turn gait, rising-from-a-chair, and a squat were simulated using both surrogate and reference contact models. Compared to the reference contact model, the surrogate contact model predicted TF forces with a root-mean-square error (RMSE) lower than 10 N and TF moments lower than 0.3 Nm over all simulated activities. Secondary knee kinematics were predicted with RMSE lower than 0.2 mm and 0.2 degrees. Simulations that used the surrogate contact model ran on average three times faster than those using the reference model, allowing the simulation of a full gait cycle in 4.5 min. This modeling approach proved fast and accurate enough to perform extensive parametric analyses, such as simulating subject-specific variations and surgical-related factors in TKR.*

KEYWORDS

TKR, TKA, surrogate model, contact, musculoskeletal model

INTRODUCTION

The calculation of forces acting on the musculoskeletal (MS) system during activities of daily living (ADLs) is of great interest as it aids in understanding how hard and soft tissues interact throughout the human body and at the joint level, and may help researchers and clinicians to understand better the mechanical pathways of MS pathologies. Body-level forces and moments are solved using multi-rigid body dynamic methods, which are normally inexpensive computationally: given a known motion and the external forces acting on the body, muscle and joint forces can be calculated by means of forward dynamics assisted data tracking and inverse dynamics with optimization-based muscle recruitment. The reader is referred to ref. [1] for an extensive review of these techniques. At the joint and tissue level, more advanced techniques – such as finite-element (FE) or elastic-foundation (EF) analyses – are required to represent the contact interactions between articulating surfaces and solve for ligament forces and secondary motions of the joints.

Despite its great appeal, the coupling of such techniques for solving tissue-level and body-level mechanics is overall a highly computationally demanding process, up to a point that may hinder its clinical applicability or impede parametric and/or optimization analyses on a large scale. Recently, the force-dependent kinematic (FDK) method [2] was applied to estimate leg muscle forces, knee ligament and contact forces and secondary kinematics simultaneously in a MS model of a patient having a total knee replacement (TKR) [3]. However, the computational burden in that study was considerable, as it took more than four hours to analyze a single cycle of normal gait.

Surrogate models have been proposed to reduce the computational burden of MS simulations while retaining a reasonable level of accuracy. Halloran et al. demonstrated adaptive surrogate modeling techniques to accelerate the optimization of a jump height in a combined MS-FE model of the foot [4]. Surrogate models for the analysis of native knee joint forces [5,6], cartilage stresses [7] and tibiofemoral (TF) contact interactions and wear in total knee replacement (TKR) [8–11] were also reported. These models utilized a variety of techniques, such as response surface optimization [6], Lazy Learning [4], nonlinear dynamic models [5], Kriging [8–10], and artificial neural networks (ANN) [5,7,11]. Recently, Eskinazi and Fregly (2015) proposed a surrogate modeling approach based on ANN to accelerate an FE deformable contact model of TKR [11]. Artificial neural networks are known, among others, for their ability to learn virtually any complex relationship between a set of input and output variables [12]. For instance, for the knee joint, one would train ANNs using outcomes of repeated contact analyses of expensive reference FE or EF models, and subsequently fit the relationships between TF pose and the resultant TF contact forces and moments. Then, within a musculoskeletal analysis, the surrogate model would replace the reference contact model, providing a significant reduction in computation time. However, the performance of surrogate contact models for the simultaneous estimation of muscle forces, TF ligament and contact forces and secondary kinematics during activities of daily living (ADLs) has not been demonstrated yet.

The aim of this study is to create and test a surrogate contact model of a TKR and to demonstrate its applicability in predicting muscle, ligament and TF contact forces and

secondary kinematics simultaneously during normal gait, right-turn gait, rising-from-a-
110 chair, and squat. We addressed the following specific questions: 1) how much reduction in simulation time is obtained and 2) how well is accuracy retained when a surrogate
112 contact model is used instead of the reference contact model?

114 **METHODS**

116 A previously validated patient-specific MS model of a patient with a telemetric knee prosthesis was the basis for this study [3]. The model was built using the AnyBody
118 Modeling System (AMS, version 6, AnyBody Technology A/S, Aalborg, Denmark) [13] and included head, two arms, trunk, pelvis and two legs. Further details can be found in ref.
120 [3]. The analysis workflow consisted of two stages: a motion optimization (MO) and force-dependent kinematics (FDK), which applies inverse dynamic analysis as part of the
122 solution process. In the first stage (MO), the full-body model was driven using marker trajectories from motion-capture data, and joint kinematics were optimized using an
124 inverse kinematic analysis [14]. The AMS applies a full Cartesian formulation in which each body is described by the translation of the segment origin and the segment
126 orientation specified with Euler parameters. The relative movement between the segments is restricted by constraint equations, which, in this case, allowed three
128 translation and three rotations of the pelvis segment relative to the global reference frame, three pelvis-trunk rotations, neck extension and for each leg, three hip rotations,
130 knee flexion, ankle plantarflexion and subtalar eversion. In the second stage (FDK), the optimized joint kinematics from MO stage and the experimental ground reaction forces

and moments (GRF&Ms) were input to an FDK model, which solved for the 166 Hill-type muscle element forces spanning the lower extremity, TF ligament and contact forces, and secondary TF joint kinematics under an assumption of quasi-static equilibrium within the joint [2]. To save computation time, the right (unaffected) leg and both arms were excluded from the FDK analyses and artificial reaction forces and moments were added to the pelvis segment to compensate for kinematic-kinetic inconsistencies.

Description of the Reference Contact Model

The reference TKR contact model of a left knee used in this study was extracted from the aforementioned MS model. It consisted of two contact pairs defined by the femoral component and the medial and lateral side of the tibial insert, respectively. Implant geometries were obtained from the 5th "Grand Challenge Competition to Predict In Vivo Knee Loads" dataset [15]. TF contact forces and moments were calculated using a linear pressure-overclosure relationship between the articulating surfaces, in which the contact forces were a linear function of the penetration volume, with a factor (pressure modulus) of 9.3 GN/m^3 [3].

To generate a surrogate contact model of TKR, it was necessary to find the relationship between contact forces and moments resulting from the relative pose between the tibial and femoral component. For this, we used a design-of-experiment approach to define a model sampling scheme to obtain the desired input-output relations. Subsequently, we fitted the samples obtained from repeated evaluation of the

154 reference contact model using ANN until convergence criteria were reached. Details of this procedure are herein provided.

156 The tibial component, consisting of medial and lateral contact surfaces, was fixed to the global reference frame. The femoral component was free to move in space having 158 6 DOFs relative to the global frame. Thus, the relative TF pose could be defined by three translations and three rotations between tibial (fixed) and femoral (moving) frames of 160 reference (Fig. 1). Tibiofemoral translations were defined as the translations of the femoral component frame measured with respect to the tibial frame of reference, and 162 corresponded to anterior femur translation (*x*), joint distraction (*y*), and medial femur translation (*z*), respectively. Tibiofemoral rotations were defined using Tait-Bryan angles 164 with the 'z-y-x' sequence of intrinsic rotations from the femoral component body frame to the tibial component body frame. This rotation sequence allowed the description of 166 knee abduction (ϑ_x) around a well-defined axis fixed in the tibial body. As will become clearer in the next section, knee abduction was a sensitive rotation, therefore, it was 168 allowed to vary according to the abduction torque applied. Letting knee abduction be the last rotation in the sequence, a change in the rotation did not affect the remaining 170 two non-sensitive rotations (ϑ_z and ϑ_y). Please note that the used sequence ('z-y-x' rotations from femur to tibia) is equivalent to a 'x-y-z' rotation sequence from tibia to 172 femur, as defined in ref. [11], with an opposite sign convention. Furthermore, the assumptions of conservative (friction-less) and linear elastic contact were made. Under 174 these conditions, it was possible to simplify the contact formulation and assume the contact forces and moments to depend purely on TF pose. Tibio-femoral forces and

176 moments resulting from medial and lateral contact analyses were measured with respect to the origin of the femoral coordinate system and expressed in the tibial
178 reference frame. They will be referred to as F_x^{Med}, F_y^{Med}, F_z^{Med}, M_x^{Med}, M_y^{Med}, M_z^{Med}, for the medial side, and F_x^{Lat}, F_y^{Lat}, F_z^{Lat}, M_x^{Lat}, M_y^{Lat}, M_z^{Lat}, for the lateral side, in which the
180 subscripts indicate the direction of application of the load. The resultant forces and moments from the medial and lateral sides combined could be conveniently expressed
182 as the total TF loads: F_x^{Tot}, F_y^{Tot}, F_z^{Tot}, M_x^{Tot}, M_y^{Tot}, M_z^{Tot}.

184 **Sampling of the Reference Contact Model**

186 An efficient sampling plan was necessary to ensure coverage of the design space. Ideally, the surrogate model should have a perfect fit in all areas of the design space,
188 which are likely to occur in a simulation, and also adequate in less probable areas, in order to prevent the contact algorithm from producing unacceptably large prediction
190 errors. Due to the particular geometry of the articulating surfaces in TKR, there are specific directions in which minimal variations of the TF pose induce very large
192 variations in the corresponding TF loads. These are referred to as 'sensitive directions' [8]. To identify possible sensitive directions in our contact model, we configured a
194 reference TF pose in which all rotations and the anterior and medial femur translation were null and the femoral component "just touched" the tibial component.
196 Subsequently, we perturbed the TF pose and analyzed the TF load response. We identified two sensitive directions, being the joint distraction (y) and the knee abduction
198 (ϑ_x), respectively. The presence of sensitive directions suggested a definition of sample points as combinations of pose parameters in non-sensitive directions and loads in

200 sensitive directions: {x, F_y^{Tot}, z, M_x^{Tot}, ϑ_y, ϑ_z}, as in [8]. This definition was adopted to sample two-sided contact and contact boundary cases. To ensure a wider coverage of
202 the design space, one ought to include also out-of-contact and single-sided contact cases [11]. In such cases, we adopted different definitions of the sample point, namely
204 {x, y, z, ϑ_x, ϑ_y, ϑ_z} for out-of-contact cases, for which the femoral component could be freely moved far away from the tibial insert, and {x, F_y^{Tot}, z, ϑ_x, ϑ_y, ϑ_z} for single-sided
206 contact cases, for which the knee abduction angle could be explicitly prescribed so as to produce lift-off on either sides, as in [11].

208 To define reasonable boundaries for the design space, we estimated and extracted TF load-pose data from five reference FDK analyses of ADLs obtained using
210 our MS model with the reference contact model. These activities included one walking cycle of normal gait, one of right-turn gait, an unloaded leg-swing, two repetitions of a
212 rising-from-a-chair task, and four repetitions of a squatting motion, for which motion-capture data were available as part of the Grand Challenge dataset [15]. Differently than
214 in the study of Eskinazi and Fregly [11], in which reference curves were extracted from 14 gait cycles, we included reference curves from several types of ADLs, with the aim of
216 generalizing the capabilities of the surrogate contact model for future use, as we plan to apply the surrogate model in MS analyses involving different loading conditions and
218 ranges of motion.

To take into account different contact cases, we adopted a multi-domain
220 approach, as in the study of Eskinazi and Fregly [11], and we chose the Hammersley quasi-random (HQ) sequence [16] to evenly distribute points in each domain (Table 1).

However, some different choices were made for distributing samples points across domains, as detailed below. By using multiple domains, we attempted to maximize the coverage of areas of the design space that are as likely to occur as normal two-sided contact during the analysis of ADLs, for instance including lift-off of one or both of the two sides of the implant, or situations where the implant surfaces are barely in contact. Domain 1 consisted of data points spanning the boundaries of ± 1 standard deviation (SD) from the time-varying envelopes of each of the aforementioned reference analyses. This domain compared to domains D1 and D2 in the study of Eskinazi and Fregly [11], with the differences being the expansion factor of 1 SD (our method) as opposed to 20 % and 100 % (their method), and the fewer points sampled. For each time-frame, 20 data points were sampled, resulting in 18060 points. Our Domain 2 was comparable to domain D3 in ref. [11], though the sampling process was different. We first performed a principal component analysis (PCA) of the reference data, then we enlarged the envelopes of the principal components (PCs) by 50 % and we sampled data points in the new PC space. Finally, we transformed the PC samples back to the original variables space. By pre-transforming the domain space using PCA, the resulting samples points were more densely distributed around the data points of the reference curves. This domain enlarged substantially the coverage with respect to the Domain 1, while still retaining the gross inter-variability between the sampling variables, owing to PCA pre-transformation. Domain 3 represented single-sided contact, similarly to domain D4 in ref. [11], which simulated lift-off of one of the two sides of the implant. The sampling point was defined as $\{x, F_y^{Tot}, z, \vartheta_x, \vartheta_y, \vartheta_z\}$. Differently than in ref. [11], the PCA approach

was used for the TF pose parameters and an upper boundary equal to 100 N was set on F_y^{Tot} (lower boundary was 0 N), which covered situations with low contact forces on either sides. Domain 4 consisted of contact boundary points, similar to domains D6 and D7 in ref. [11], in which one or both sides were barely touching. This domain accounted, for instance, for situations in which the leg would enter the swing phase of gait, and the TF loads would progressively decrease. The sample point definition for this domain was $\{x, F_y^{Tot}, z, M_x^{Tot}, \vartheta_y, \vartheta_z\}$, thus we set an upper boundary of 100 N on F_y^{Tot}, and a lower and upper boundary of ± 5 Nm on M_x^{Tot}. This choice differed from that of Eskinazi and Fregly for domain D6 and D7, in which the medial and lateral vertical contact forces were kept fixed at 5 N, simultaneously or alternately, while sampling the TF pose parameters. Domains 5 and Domain 6 were populated with samples representing both sides out-of-contact cases, in which the femoral component was in the proximity (Domain 5) and far away (Domain 6) from the tibial insert, respectively. The sample point definition was $\{x, y, z, \vartheta_x, \vartheta_y, \vartheta_z\}$. Our Domain 5 was comparable to domain D5 in ref. [11], but we sampled a much larger number of points. In this domain, the contact boundary samples were re-used, and the distraction was raised up to 2 mm in four increments (as opposed to three in ref. [11]). Furthermore, we extended the out-of-contact coverage with Domain 6, to ensure that the response of the surrogate model did not diverge dramatically when the femoral component separated substantially from the tibial component, providing additional robustness to the surrogate model. In Domain 6, boundaries on the *y* translation were set between the maximum *y* translation of contact boundary cases and 10 cm.

All sample points were evaluated by repeated static analyses using the reference contact model (Fig. 1), to obtain the combinations of TF pose and corresponding TF loads. As for Domains 5 and 6 – in which samples consisted purely of pose parameters – the analysis was displacement-driven and TF loads solved for using ordinary inverse dynamics. Sampling domains that included sensitive directions for certain loads (Domains 1-to-4) were analyzed using a combination of displacement-driven and force-driven analyses, where TF pose parameters in non-sensitive directions and loads in sensitive directions were prescribed, whereas TF pose parameters in sensitive directions and loads in non-sensitive directions were simultaneously solved for using FDK analyses. In these cases, the FDK algorithm solved for the unknown TF pose parameters in sensitive directions that put the system in static equilibrium, under the application of TF loads in sensitive directions and the prescribed pose in non-sensitive directions. Errors of up to 0.1% of the applied loads were tolerated, whereas samples that led to larger errors were discarded. Additionally, samples that led to TF component overclosure larger than 2 mm were also filtered out. Approximately 85% of all the successful sample points were allocated for surrogate model training. The remaining 15% were assigned to a separate testing dataset. No samples were allocated for testing in Domain 1, as the accuracy in this sort of domain would be better evaluated by FDK analysis of ADLs.

Training of the Surrogate Contact Model

Multiple-input multiple-output feedforward ANNs were configured in MATLAB (version 8.6.0, The MathWorks Inc., Natick, MA) using the Neural Network Toolbox (Fig. 2). As opposed to the study of Eskinazi and Fregly, who interconnected multiple ANNs, each

290 with multiple inputs and a single output [11], we opted for ANNs with multiple inputs and multiple outputs in an attempt to exploit the correlation likely to exist between
292 different output variables. Similarly to ref. [11], the training phase consisted of two stages: in the first stage, one ANN learned the relationship between medial and lateral
294 TF loads in sensitive directions, $\{F_y^{Lat}, M_x^{Lat}, F_y^{Med}, M_x^{Med}\}$, and the TF pose, $\{x, y, z, \vartheta_x, \vartheta_y, \vartheta_z\}$; in the second stage, two additional ANNs learned the relations between the
296 remaining medial and lateral TF loads separately, and a combination of TF pose parameters and sensitive loads of either side. This allowed proper learning of the out-of-
298 contact cases, in which zero loads may correspond to many different combinations of pose parameters and to have fully independent medial and lateral surrogate contact
300 models.

Given the impossibility to establish *a priori* the correct number of layers and
302 neurons, a heuristic method was used to decide both number of network layers and neurons per layer. We started with two hidden layers and ten neurons per layer. We
304 started the network training and recorded the value of the performance function after one hour. If the performance value fell below 0.001, then we would accept the current
306 network configuration, else we would primarily add ten neurons to each layer (up to forty neurons in total per layer) and, secondly, add one more hidden layer. After each
308 network modification we would repeat the one-hour training test. This process led us to a final network configuration consisting of three hidden layers with thirty neurons per
310 layer, having hyperbolic tangent sigmoid transfer function. The network was then completed with one output layer of purely linear neurons.

Each network was trained using the MATLAB training function `trainbr`, which uses Bayesian regularization within the Levenberg-Marquardt backpropagation algorithm. According to this training scheme, the performance function to be minimized was a linear combination of squared errors and weights, in which the coefficients were continuously updated to prevent data over-fitting and lead to networks with good generalization qualities. Each network trained for at least 18 hours and the training was stopped only after the performance function visibly converged.

After training succeeded, the weights and biases of each network were exported as standalone functions using built-in MATLAB capabilities. Custom-written MATLAB routines translated those standalone functions into C++ code. The Eigen template library [17] was used to represent and operate on numerical data in the C++ surrogate model functions. The latter were then built together as a dynamic-link library (DLL) to maximize efficiency. A post hoc condition was defined in the surrogate model functions: if the medial or lateral TF force in the *y* direction was negative or equal to zero, then all remaining loads on the respective side were immediately assigned zero as well, without calculating the output of the second stage.

Testing of the Surrogate Contact Model and Performance of Simulated ADLs

We used the surrogate contact model functions to evaluate the sample points from the testing dataset, and reported the testing performances using the coefficient of determination (R^2, defined by 1 - sum of squares of residuals divided by total sum of squares) and the root-mean-square error (RMSE) of output medial and lateral TF loads relative to targets.

We then replaced the reference contact model of the MS model with the newly built surrogate contact model. This was achieved using C++ hook capabilities of the AMS, which can load external DLL functions and make them available to the model during run time. In this way, the medial and lateral TF contact loads were obtained by executing function calls to the respective medial and lateral surrogate model DLL functions, using the current TF pose as input argument. Differently from our previous MS model [3], in which the computation of muscles and ligament lines of action – or wrapping algorithm – was carried out using numerical methods, in this study, we opted for an analytical solution[2], to prevent possible hindrances to the true performances of the surrogate model. Moreover, since we were interested in testing a surrogate model of a TKR TF joint, we replaced the patellofemoral (PF) joint with an ideal revolute joint and let the only DOF of patella be controlled by an elastic patellar ligament (stiffness 1187 N/mm). During an analysis, the FDK algorithm explored the TF pose space until a quasi-static equilibrium was reached, and to do so it iteratively executed function calls to the surrogate model, rather than executing function calls to the reference contact model. To evaluate the performance of the surrogate contact model for the analysis of dynamic motor tasks, we simulated four ADLs using both the reference and the surrogate contact model. We simulated one walking cycle of normal gait, one of right-turn gait, two repetitions of a rising-from-a-chair task, and four repetitions of a squatting motion for which motion capture data were available as part of the Grand Challenge dataset [15]. For each activity and for each contact model, we estimated TF

[2] The algorithm for the analytical solution is not part of the AMS release and it was provided separately to us by AnyBody Technology A/S in a prototype version that solved a single cylindrical wrapping case.

forces, moments and six-DOF knee kinematics and we evaluated the accuracy of the surrogate model predictions compared to the predictions obtained with the reference model. We calculated R^2, RMSE, and maximum prediction errors for all TF forces, moments, and kinematics. Knee kinematics were defined according to a knee joint coordinate system consistent with the description of Grood and Suntay [18]. Tibiofemoral rotations were defined using Tait-Bryan angles with the 'z-x-y' sequence of intrinsic rotations from the femoral component body frame to the tibial component body frame. Note that this convention differed from that used during the sampling process; however, this choice was justified to provide a physically meaningful description of knee kinematics; namely, anterior tibial translation, joint distraction, lateral tibial translation, knee flexion, knee adduction, and tibial external rotation. Additionally, we compared the computation times required to complete the FDK analyses with either contact model.

RESULTS

On the testing dataset, the surrogate model predicted medial and lateral TF loads with an R^2 value greater than 0.99 and 0.96, respectively, for all components of force and moment. The largest medial and lateral RMS force errors (Table 2) were observed in F_y^{Lat} (76 N, Domain 6) and F_y^{Med} (20 N, Domain 3), respectively. The largest medial and lateral RMS moment errors were observed in M_x^{Med} (0.72 Nm, Domain 6) and M_x^{Lat} (1.9 Nm, Domain 6). Maximum errors were in most cases one to two orders of magnitude larger than RMS errors, indicating the presence of extreme outliers. The

largest maximum errors were 1863 N in F_y^{Lat} and 50 Nm in M_x^{Lat}, both found on Domain 2.

On the simulations of normal gait, right-turn gait, rising-from-a-chair, and squat, medial and lateral TF loads were predicted with an R^2 value greater than 0.99 and 0.98 in all cases. The knee kinematics obtained with the surrogate model agreed to those obtained with the reference model with an R^2 value greater than 0.96 in all cases, except for lateral tibial translation in the normal gait ($R^2 = 0.93$). The largest RMS errors among all trials (Table 3) were 5.6 N in F_y^{Med} and 9.9 N in F_y^{Lat}, and 0.17 Nm in M_x^{Med} and 0.26 Nm in M_x^{Lat}. The largest maximum errors on TF loads were 47 N for F_y^{Lat} in the right-turn and 1.4 Nm for M_x^{Med} in the normal gait. The largest RMS errors in knee kinematics (Table 4) were found in lateral tibial translation (0.13 mm) and tibial external rotation (0.17 degrees) in the right-turn. Maximum errors reached up to 0.90 mm for anterior tibial translation and up to 1.27 degrees for tibial external rotation, both in the right-turn.

Simulation times (Table 5) were 4.5 and 13.6 min for the normal gait, 7.3 and 22.7 min for the right-turn trial, 27.2 and 70.3 min for the rising-from-a-chair trial, and 38.5 and 96.4 min for the squat trial, when using the surrogate and reference contact model, respectively. The speed improvement introduced by the surrogate model was greater than 2.5 times for the squat and rising-from-a-chair trials, and greater than 3 times for the normal gait and right-turn trials, thus it was greatest in trials with a short duration and a fewer number of time frames analyzed (less than 2 s/200 frames), as opposed to trials with a longer duration (more than 8 s/1000 frames).

DISCUSSION

In this study, we successfully incorporated a surrogate contact model of a TKR based on ANNs into a MS model that solved for lower extremity muscle, TF ligament and contact forces and secondary TF kinematics simultaneously. Tibiofemoral contact forces and moments and secondary kinematics were predicted almost as accurately as with the reference contact model in all ADLs, but within a third of the time. The ability to reduce the computation time of MS analyses is an important step forward towards the application of MS models in extensive parametric studies and/or the planning of orthopedic interventions through optimization.

The prediction errors remained low across the different ADLs analyzed and among different components of the loads. For instance, RMS errors on TF compressive forces were on average less than 1% of peak forces reported for gait [19]. The RMS and maximum errors were lower than 10 N/0.26 Nm and 47 N/1.4 Nm for all load components, respectively. The sampling scheme based on multiple domains proved thus effective in providing a good coverage for the contact conditions arising during the ADLs simulated.

The RMS errors for the prediction of TF contact forces and moments during gait simulations (1.9 N/0.063 Nm) were on the same order of magnitude but slightly lower than the errors reported by Eskinazi and Fregly (2.6 N/0.078 Nm) [11]. Sub-millimeter and sub-degree accuracy was also achieved in predictions of secondary knee kinematics in all ADLs investigated, indicating that the iterative process that computed the quasi-

static equilibrium in the secondary knee DOFs converged to very similar results.

426 Moreover, when the goal is to capture the overall kinematics for various ADLs, as was in the current study, small errors in the TF loads predicted by the surrogate model do not

428 critically affect the kinematic results of the simulations. None of the previous studies reported on the accuracy of secondary knee kinematics predicted concurrently with

430 muscle, ligament and contact forces using a surrogate TF contact model.

The time to complete an FDK analysis of the ADLs investigated in this study was

432 reduced by about three times when the surrogate contact model replaced the reference contact model. The speed improvement appeared quite modest and warranted further

434 exploration. To exclude possible hidden overhead within the surrogate model functions, we investigated the execution time of isolated surrogate contact model function calls:

436 this was on the order of 77 μs per evaluation, as opposed to 78 ms for the reference contact model. Thus, at the level of isolated function calls, the surrogate model was

438 about 1000x faster than the reference contact model, as expected, however such a speed improvement did not extend to FDK analyses of ADLs. This can be explained by

440 other time-consuming processes taking place within such analysis; namely, the kinematic analysis, and the optimization that solved the muscle recruitment problem.

442 Both processes were solved numerically using iterative algorithms which themselves added overhead. Replacing the reference contact model with a faster surrogate contact

444 model removed a part of this overhead.

A full gait cycle could be analyzed in just 4.5 min, using a surrogate contact

446 model, which is of practical advantage in many cases. Extensive parametric studies often

require repeating similar analyses hundreds or thousands of times to assess the
448 influence of individual parameters. For instance, it could be interesting to study the performances of a certain implant design under varying subject-specific factors, such as
450 height, weight, muscle strength, soft tissue characteristics, and limb alignment and/or implant related factors, such as implant alignment. In all these cases, very low
452 computation times would be highly beneficial, as it would eliminate an important bottleneck in the implementation of such analyses.

454 The simulation time to analyze one walking cycle of normal gait (4.5 min) was almost one order of magnitude smaller than the time reported by a previous study that
456 used surrogate contact models of both TF and PF joints (42 min) [9]. Our model did not include a PF joint contact model; however, it included 166 Hill-type muscles elements
458 spanning the entire lower extremity, in addition to TF ligaments and contact forces, as opposed to the other study, which included only eleven muscles spanning the knee joint
460 and omitted all knee ligaments except the patellar ligament [9]. Other studies which did not employ surrogate models reported simulation times to complete a forward and
462 inverse dynamic analysis of one walking cycle which were comparable to ours (a few to ten minutes) [20–22]. However, these models did not include muscles and some
464 motions were input to the simulations; namely, knee anterior-posterior translation and internal-external rotation. The analysis approach of the present study solved for the
466 muscle forces of the entire lower extremity and did not prescribe any of the secondary knee kinematics. We believe that estimating muscle, ligament and joint contact forces
468 and secondary knee kinematics simultaneously – rather than prescribing or neglecting

any of them – is essential if the aim is to investigate the effect of implant-related factors on the overall joint function, as any of the aforementioned outcomes may affect and/or be affected by the different implant conditions. Thus, when the higher computational complexity of our modeling approach is taken into account, the time performances appear more than justified.

When evaluating the surrogate model over a testing dataset, RMS prediction errors were all lower than 76 N (F_y^{Lat} on Domain 6) and 1.9 Nm (M_x^{Lat} on Domain 6). The presence of extreme outliers was also noted, as testified by maximum errors in certain domains that were orders of magnitude higher than the RMS errors in those domains: 1863 N for F_y^{Lat} and 50 Nm for M_x^{Lat}, both on Domain 2. This signifies the presence of tiny areas of the design space that the surrogate model could not learn accurately enough and for which it produced large errors. This could have happened if, for instance, too few sample points were available in those areas during training of the surrogate model, resulting in large testing errors, or if an insufficient number of hidden layers was used in the ANN. A careful inspection of the 'problematic' points revealed that the corresponding pose parameters referred to non-physiological situations, with the femoral component almost below the tibial insert and/or rotated to a very large extent. Such cases are very unlikely encountered in realistic contact situations, and, therefore, they should not constitute a serious problem. If we exclude from the comparison our Domain 6, which does not have an analogous in a previous study [11], then the largest errors were found on analogous domains in both studies; namely, our Domain 2 and their domain 'D3', which represented an expansion of the global

reference curves. In these analogous domains, the largest RMS (maximum) errors in our study were 69 N/1.8 Nm (1863 N/50 Nm) as opposed to 14 N/0.4 Nm (249 N/4.7 Nm) in [11]. Thus, our RMS (maximum) errors were up to five (ten) times larger, which could be due to the different sampling choices (we used an expansion factor that was twice as large) and/or different surrogate model architectures.

A surrogate contact modeling toolbox (SCMT) for the creation of surrogate contact models was recently presented and made freely available by Eskinazi and Fregly [23]. This toolbox was tested for the replacement of an EF contact model of both TF and PF joints in a TKR model. In this study, we developed our own surrogate model creation process, as the reference contact model of TKR was already available, as part of a previously published MS model validated against knee forces and kinematics [3]. Furthermore, the previously published toolbox could not easily connect to our modeling environment, which let us pursue the development of a dedicated surrogate model creation process.

Our surrogate modeling approach introduced some novel aspects, as compared to previous studies, which are worth discussing. First, an advantage of the used FDK approach is that it eliminates the sensitivity of predicted muscle, ligament, and joint contact forces to errors in the location of a fixed knee flexion-extension axis when such is assumed in the applied knee model. When a fixed knee flexion-extension axis is used, typically only muscle forces are assumed to contribute to the net joint moment about the fixed axis, whereas the contribution from contact and ligament forces are neglected. Using FDK, the joint DOFs are left free to equilibrate under the compound action of

muscle, ligaments and contact forces (in a quasi-static fashion) and no assumptions are required about the DOFs to which contact (and ligament) forces do not, and do, contribute. This methodology relieves very much the efforts when modeling complex non-conforming joints, such as the knee [2]. Second, pre-transforming the sampling variables using PCA in Domain 2 and Domain 3 likely made our sampling scheme more efficient, as the resulting sample points could be more densely distributed close to the data points from the reference curves. This is due to the PCA being able to decouple the original variables, thus allowing sampling along the principal directions of the reference data points. Third, although an explicit comparison was not performed in this study, choosing multiple-output instead of single-output ANNs may have benefitted the final accuracy, as the covariance existing between the output loads was taken into account during the fitting process, whereas single-output ANNs would fit each of the output variables independently from the others. However, this should be investigated in a future study. Fourth, using Bayesian regularization as part of the ANN training algorithm helped preventing data over-fitting and producing ANNs with good generalization qualities. Using a training algorithm that does not intrinsically over-fit the data has also the practical advantage of not requiring a constant monitoring of the training state and/or an additional dataset on which to perform validation.

We should note that our surrogate model creation process is not limited uniquely to the contact model presented in this study, but can be easily extended to virtually any other FE or EF contact models, provided that the assumptions of elastic and friction-less contact are met. In that respect, the surrogate model could provide a fast

and valid alternative to contact models which cannot directly interface to the modeling system of use. Furthermore, the surrogate model resulting from our creation process can be exploited in virtually any simulation software capable of integrating an external DLL module. This represents a very viable way to describe complex structural models, without actually simulating them.

The time required to generate the sample points amounted to almost 5 days of continuous computation on all four cores of an Intel® Core™ i5-4570 quad-core CPU equipped with 16 gigabytes of RAM. About 60 additional hours were necessary to train the ANNs. The total surrogate model generation time was considerable, however, both the sampling process and the training of the neural networks could be massively parallelized and executed on multiple processing units, or machines with many cores. This approach would easily bring the generation time to more manageable levels. It should also be noted that the generation time for a given implant design is paid only once upfront, but the resulting surrogate model can be reused for the evaluations of many conditions and multiple patients. Another way to reduce the generation time would be to reduce the number of training points, but this aspect requires further investigation.

The sample generation process relied heavily on reference curves and/or variables bounds extracted from existing reference simulations performed with the reference model. This approach may work well when such data are already available – or if they can easily be obtained from experimental measurements – however, this is seldom the case. Perhaps the most challenging case is that of a patient-specific knee

model, generated *ex novo* from medical images of the patient. In such a case, although some joint kinematics may be extracted using *in vivo* imaging techniques, no reference load curves are available and a different sampling strategy should be devised. The definition of bounds for the sample points could also be based on the geometrical conformity between the articulating surfaces, and bounds on joint loads in sensitive directions could be obtained from the literature. However, these approaches require further investigation.

The activities simulated in this study were also incidentally used during the sampling stage to provide reference curves. If activities were to be simulated which involved joint loads and/or kinematics very different from the ones in the training dataset, it is almost impossible to know whether the surrogate model predictions would still be sufficiently accurate. One possible solution could be to build accuracy maps over various regions of the design space and, subsequently, to relate the distance of new query points from the dataset of training points prior to the surrogate model evaluation to estimate the expected accuracy for the new points. However, mapping the accuracy over a multi-dimensional domain is not trivial.

We introduced a discontinuity in the surrogate model, which prevented negative forces in the TF distraction (y) direction, and avoided the estimation of TF loads in non-sensitive directions when the compressive force was lower than or equal to zero. To find the configuration of static equilibrium in the TF joint, the FDK method solves a set of nonlinear equations using gradient information. Therefore, our choice made the gradient of the system of equations potentially discontinuous, whereas a smooth

transition to zero would be a better choice. However, the reference contact model contained the same discontinuity and the surrogate contact model did not exacerbate this problem.

Friction between the articular implant surfaces was neglected and the contact was assumed to be linear elastic based on penetration volume. The friction-less assumption may not allow proper study of polyethylene wear of the tibial insert under dynamic conditions. However, for all other cases of interest (e.g., parametric variation, knee kinematic studies and ligament force predictions), this assumption does not represent a major limitation. With regards to the linear elastic assumption, previous studies have failed to demonstrate the superiority of non-linear contact models over linear models to describe the load response of the polyethylene component [24]. However, the surrogate contact model creation process should work just as well for non-linear elastic contact models, as long as the contact forces and moments can be represented as functions of only model pose.

In conclusion, we successfully applied surrogate modeling techniques based on ANNs to reduce the computation time of knee joint loads and kinematics in MS models. We evaluated its accuracy and demonstrated its performance in the simulation of four ADLs. Accuracy was comparable to that of the reference model, while simulations were performed three times as fast, with a full gait cycle analyzed in only 4.5 min. We believe that these performances will promote the applicability of MS models in extensive parametric studies and/or planning of orthopedic interventions through optimization.

602 **FUNDING**

604 The research leading to these results has received funding from the European Research Council under the European Union's Seventh Framework Programme
606 (FP/2007-2013) / ERC Grant Agreement n. 323091 awarded to N. Verdonschot. This work was also supported by the Danish Council for Independent Research under grant
608 n. DFF-4184-00018 to M. S. Andersen. Finally, contributions by M. Damsgaard, AnyBody Technology, were funded by the European Union's Seventh Framework Programme
610 under grant agreement n. NMP-310477 and the Innovation Fund Denmark.

REFERENCES

[1] Erdemir, A., McLean, S., Herzog, W., and van den Bogert, A. J., 2007, "Model-based estimation of muscle forces exerted during movements.," Clin Biomech (Bristol, Avon), **22**(2), pp. 131–54.

[2] Andersen, M. S., Damsgaard, M., and Rasmussen, J., 2011, "Force-dependent kinematics: a new analysis method for non-conforming joints," XIII International Symposium on Computer Simulation in Biomechanics, Leuven, Belgium.

[3] Marra, M. A., Vanheule, V., Fluit, R., Koopman, B. H. F. J. M., Rasmussen, J., Verdonschot, N., and Andersen, M. S., 2015, "A subject-specific musculoskeletal modeling framework to predict in vivo mechanics of total knee arthroplasty.," J Biomech Eng, **137**(2), p. 20904.

[4] Halloran, J. P., Erdemir, A., and van den Bogert, A. J., 2009, "Adaptive surrogate modeling for efficient coupling of musculoskeletal control and tissue deformation models.," J Biomech Eng, **131**(1), p. 11014.

[5] Mishra, M., Derakhshani, R., Paiva, G. C., and Guess, T. M., 2011, "Nonlinear surrogate modeling of tibio-femoral joint interactions," Biomed Signal Process Control, **6**(2), pp. 164–174.

[6] Lin, Y.-C., Farr, J., Carter, K., and Fregly, B. J., 2006, "Response surface optimization for joint contact model evaluation.," J Appl Biomech, **22**(2), pp. 120–30.

[7] Lu, Y., Pulasani, P. R., Derakhshani, R., and Guess, T. M., 2013, "Application of neural networks for the prediction of cartilage stress in a musculoskeletal system.," Biomed Signal Process Control, **8**(6), pp. 475–482.

[8] Lin, Y.-C., Haftka, R. T., Queipo, N. V, and Fregly, B. J., 2010, "Surrogate articular contact models for computationally efficient multibody dynamic simulations.," Med Eng Phys, **32**(6), pp. 584–94.

[9] Lin, Y.-C., Walter, J. P., Banks, S. A., Pandy, M. G., and Fregly, B. J., 2010, "Simultaneous prediction of muscle and contact forces in the knee during gait.," J Biomech, **43**(5), pp. 945–52.

[10] Lin, Y.-C., Haftka, R. T., Queipo, N. V, and Fregly, B. J., 2009, "Two-dimensional surrogate contact modeling for computationally efficient dynamic simulation of total knee replacements.," J Biomech Eng, **131**(4), p. 41010.

[11] Eskinazi, I., and Fregly, B. J., 2015, "Surrogate modeling of deformable joint contact using artificial neural networks.," Med Eng Phys, **37**(9), pp. 885–91.

[12] Hornik, K., Stinchcombe, M., and White, H., 1989, "Multilayer feedforward networks are universal approximators," Neural Networks, **2**(5), pp. 359–366.

[13] Damsgaard, M., Rasmussen, J., Christensen, S. T., Surma, E., and de Zee, M., 2006, "Analysis of musculoskeletal systems in the AnyBody Modeling System," Simul Model Pract Theory, **14**(8), pp. 1100–1111.

[14] Andersen, M. S., Damsgaard, M., and Rasmussen, J., 2009, "Kinematic analysis of over-determinate biomechanical systems.," Comput Methods Biomech Biomed Engin, **12**(4), pp. 371–84.

[15] Fregly, B. J., Besier, T. F., Lloyd, D. G., Delp, S. L., Banks, S. a, Pandy, M. G., and

D'Lima, D. D., 2012, "Grand challenge competition to predict in vivo knee loads.," J Orthop Res, **30**(4), pp. 503–13.

[16] Hammersley, J. M., 2006, "MONTE CARLO METHODS FOR SOLVING MULTIVARIABLE PROBLEMS," Ann N Y Acad Sci, **86**(3), pp. 844–874.

[17] Guennebaud, G., Jacob, B., and others, 2010, "Eigen v3" [Online]. Available: http://eigen.tuxfamily.org.

[18] Grood, E. S., and Suntay, W. J., 1983, "A joint coordinate system for the clinical description of three-dimensional motions: application to the knee.," J Biomech Eng, **105**(2), pp. 136–44.

[19] D'Lima, D. D., Fregly, B. J., Patil, S., Steklov, N., and Colwell, C. W., 2012, "Knee joint forces: prediction, measurement, and significance.," Proc Inst Mech Eng H, **226**(2), pp. 95–102.

[20] Bei, Y., and Fregly, B. J., 2004, "Multibody dynamic simulation of knee contact mechanics.," Med Eng Phys, **26**(9), pp. 777–89.

[21] Fregly, B. J., Sawyer, W. G., Harman, M. K., and Banks, S. A., 2005, "Computational wear prediction of a total knee replacement from in vivo kinematics.," J Biomech, **38**(2), pp. 305–14.

[22] Fregly, B. J., Banks, S. A., D'Lima, D. D., and Colwell, C. W., 2008, "Sensitivity of knee replacement contact calculations to kinematic measurement errors.," J Orthop Res, **26**(9), pp. 1173–9.

[23] Eskinazi, I., and Fregly, B. J., 2016, "An Open-Source Toolbox for Surrogate Modeling of Joint Contact Mechanics.," IEEE Trans Biomed Eng, **63**(2), pp. 269–77.

[24] Fregly, B. J., Bei, Y., and Sylvester, M. E., 2003, "Experimental evaluation of an elastic foundation model to predict contact pressures in knee replacements.," J Biomech, **36**(11), pp. 1659–68.

Table Caption List

684

Table 1 Sampling domains, number of samples and approximate sampling time for each domain

Table 2 RMS (maximum) prediction errors of medial (*Med*) and lateral (*Lat*) TF loads for the testing dataset in each sampling domain.

Table 3 RMS (maximum) prediction errors of medial (*Med)* and lateral (*Lat*) TF loads for normal gait, right-turn, rising-from-a-chair, and squat.

Table 4 RMS (maximum) prediction errors of knee kinematic parameters for normal gait, right-turn, rising-from-a-chair, and squat.

Table 5 Simulation times and speed improvement for surrogate vs. reference contact model for normal gait, right-turn, rising-from-a-chair, and squat.

686 **Figure Captions List**

Fig. 1 Contact model of TKR. The TF pose is defined by the relative translation and rotation between the femoral component frame (blue) and the tibial component frame (red). Tibiofemoral translations are expressed in the tibial component frame of reference, and represent anterior femur translation (x), joint distraction (y), and medial femur translation (z). Tibiofemoral rotations are expressed in the femoral component frame of reference with Cardan angles using the *z-y-x* sequence of rotations, where the first rotation represent knee extension, the second, tibial external rotation, and the third, knee abduction. Rigid surface contact based on pressure-overclosure is defined between medial and lateral side of tibial component and femoral component. To obtain samples for the surrogate model, this contact model is evaluated using repeated static analyses.

Fig. 2 Diagram of the 2-stage feedforward artificial neural network (ANN). The stage I network (left) learned the relations between TF loads in sensitive directions (F_y^{Med}, T_x^{Med}, F_y^{Lat}, T_x^{Lat}) and the TF pose parameters; in stage II (right) the remaining TF loads of medial (lateral) side are obtained as functions of the TF pose and the medial (lateral) TF loads from stage I. HL: hidden layers, W: network weights, b: network biases.

Fig. 3 Medial (top) and lateral (bottom) TF compressive forces during normal

gait, right-turn, rising-from-a-chair, squat simulation. Reference measured force (eTibia, shaded), predictions using surrogate (solid) and reference (dotted) contact model.

Fig. 4 Anterior tibial translation, joint distraction, lateral tibial translation, knee flexion, knee adduction and tibial external rotation predicted using the reference contact model (solid line) and the surrogate contact model (dotted line) during normal gait, right-turn, rising-from-a-chair, and squat simulation.

688

Table 1

Domain	Description	Number of training samples	Number of testing samples	Approximate sampling time core time (effective time)[a]
1	Time-varying local envelopes of reference simulations expanded by 1 SD	18 060	-	102 (25) hours
2	Global envelopes of reference simulations expanded by 50 %	27 253	3 416	226 (57) hours
3	Single-sided contact (lift-off cases)	10 000	1 765	47 (12) hours
4	Contact boundary (swing phase)	9 990	1 755	70 (17) hours
5	Out-of-contact, proximity cases (*y* up to 2 mm, in four steps)	67 760	11 958	11 (3) hours
6	Out-of-contact, far away cases (*y* up to 10 cm, coarse)	2 000	353	15 (4) min
	Total	134 973	19 247	456 (114) hours

690 [a]Sampling time referred to a single CPU core. Considering a total of 4 cores per CPU, the effective sampling time is reduced by four.

692

Table 2

Domain	Side	F_x (N)	F_y (N)	F_z (N)	M_x (Nm)	M_y (Nm)	M_z (Nm)
2	Med	3.8 (58)	18 (462)	3.2 (32)	0.44 (9.7)	0.09 (1.4)	0.21 (6.5)
	Lat	12 (379)	69 (1863)	9.3 (315)	1.8 (50)	0.32 (11)	1.1 (41)
3	Med	3.9 (32)	20 (113)	6.8 (81)	0.46 (2.9)	0.14 (1.5)	0.21 (1.7)
	Lat	5.2 (48)	29 (191)	8.0 (126)	0.71 (5.3)	0.19 (2.3)	0.40 (6.7)
4	Med	2.1 (23)	9.9 (108)	3.9 (41)	0.26 (2.3)	0.07 (0.58)	0.12 (2.3)
	Lat	2.3 (14)	13 (77)	3.3 (49)	0.35 (2.3)	0.07 (0.51)	0.14 (1.1)
5	Med	0.13 (3.2)	1.0 (16)	0.44 (8.0)	0.03 (0.57)	0.01 (0.11)	0.01 (0.16)
	Lat	0.15 (5.3)	1.4 (25)	0.20 (5.4)	0.04 (0.42)	0.00 (0.21)	0.01 (0.15)
6	Med	8.4 (140)	17 (273)	3.2 (41)	0.72 (12)	0.13 (2.0)	0.02 (0.3)
	Lat	44 (602)	76 (1192)	51 (727)	1.9 (28)	1.8 (21)	0.77 (11)

694

696 **Table 3**

Trial	Side	F_x (N)	F_y (N)	F_z (N)	M_x (Nm)	M_y (Nm)	M_z (Nm)
Normal gait	Med	0.50 (2.2)	4.2 (14)	1.1 (11)	0.17 (1.4)	0.02 (0.09)	0.04 (0.17)
	Lat	0.50 (2.0)	4.4 (17)	0.43 (2.7)	0.12 (0.54)	0.02 (0.08)	0.01 (0.05)
Right-turn	Med	0.49 (3.0)	4.3 (24)	2.2 (11)	0.14 (0.65)	0.04 (0.18)	0.04 (0.16)
	Lat	0.95 (4.8)	9.9 (47)	2.2 (21)	0.26 (1.2)	0.03 (0.17)	0.10 (0.6)
Rising-from-a-chair	Med	0.85 (2.7)	5.6 (13)	0.51 (1.5)	0.11 (0.28)	0.01 (0.04)	0.06 (0.14)
	Lat	0.57 (2.0)	5.7 (13)	0.66 (2.1)	0.11 (0.30)	0.02 (0.07)	0.06 (0.16)
Squat	Med	0.34 (1.1)	4.2 (10)	0.51 (2.0)	0.10 (0.23)	0.01 (0.02)	0.06 (0.15)
	Lat	0.29 (0.96)	3.7 (11)	0.55 (2.2)	0.10 (0.23)	0.01 (0.04)	0.04 (0.13)

698

Table 4

Trial	*Anterior Tibial Translation (*mm*)*	*Joint Distraction (*mm*)*	*Lateral Tibial Translation (*mm*)*	*Knee Flexion (*deg*)*	*Knee Adduction (*deg*)*	*Tibial External Rotation (*deg*)*
Normal gait	0.06 (0.34)	0.01 (0.06)	0.07 (0.15)	0.00 (0.00)	0.01 (0.06)	0.04 (0.30)
Right-turn	0.12 (0.90)	0.10 (0.62)	0.13 (0.84)	0.09 (0.43)	0.14 (0.72)	0.17 (1.27)
Rising-from-a-chair	0.03 (0.16)	0.01 (0.03)	0.01 (0.08)	0.01 (0.02)	0.01 (0.06)	0.03 (0.14)
Squat	0.02 (0.10)	0.00 (0.01)	0.00 (0.03)	0.00 (0.02)	0.01 (0.02)	0.03 (0.10)

700

Table 5

Trial	Number of time-frames	Trial duration (s)	FDK simulation time		Speed improvement
			Reference model (min)	Surrogate model (min)	
Normal gait	146	1.2	13.6	4.5	3.0
Right-turn	187	1.5	22.7	7.3	3.1
Rising-from-a-chair	1066	8.8	70.3	27.2	2.6
Squat	1074	8.9	96.4	38.5	2.5

Figure 1

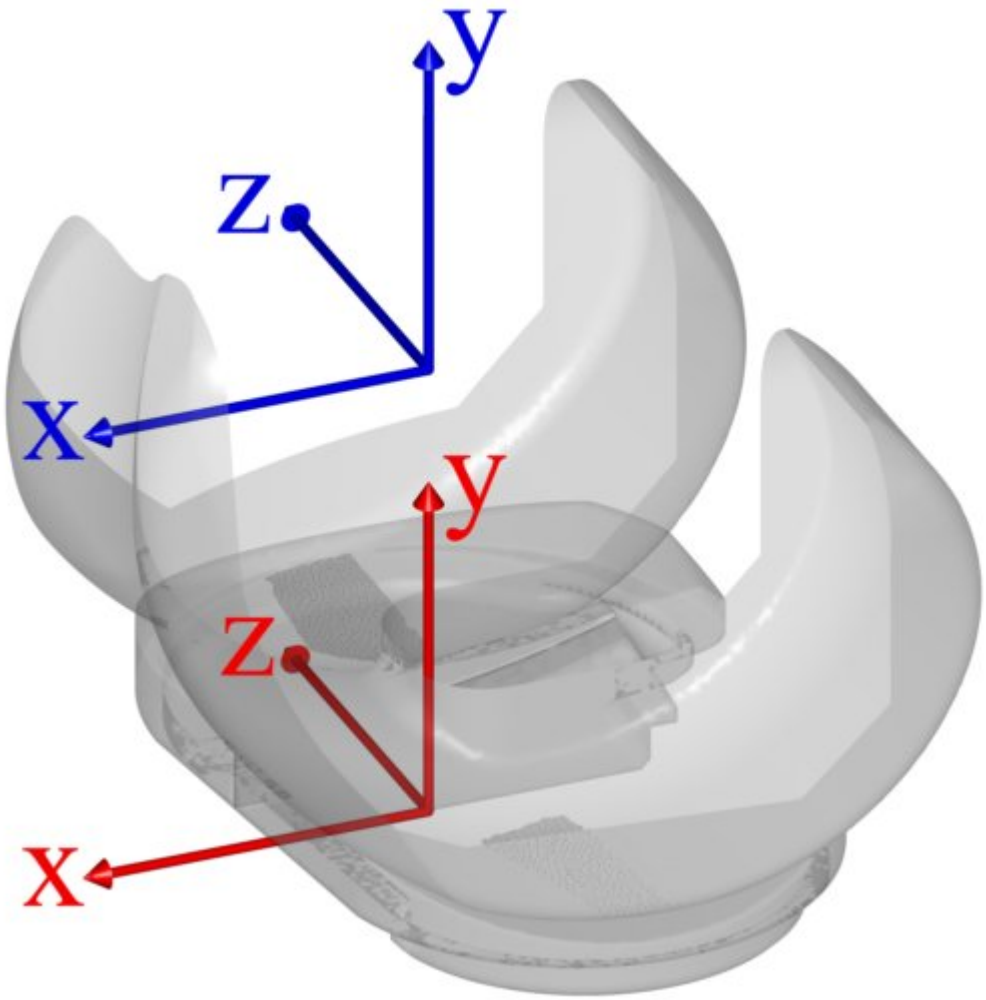

706

708 **Figure 2**

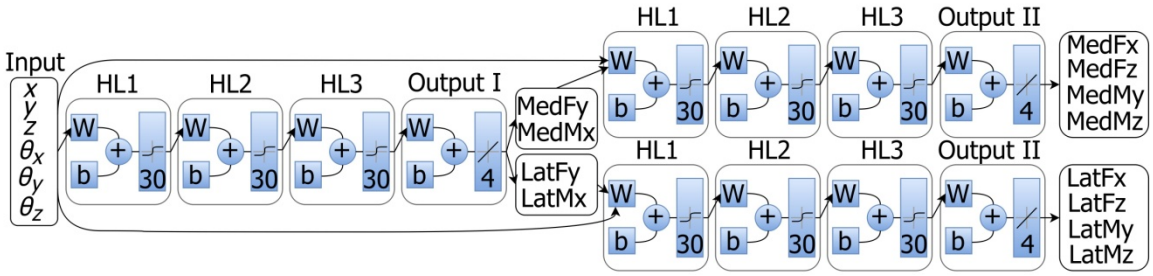

710

Figure 3

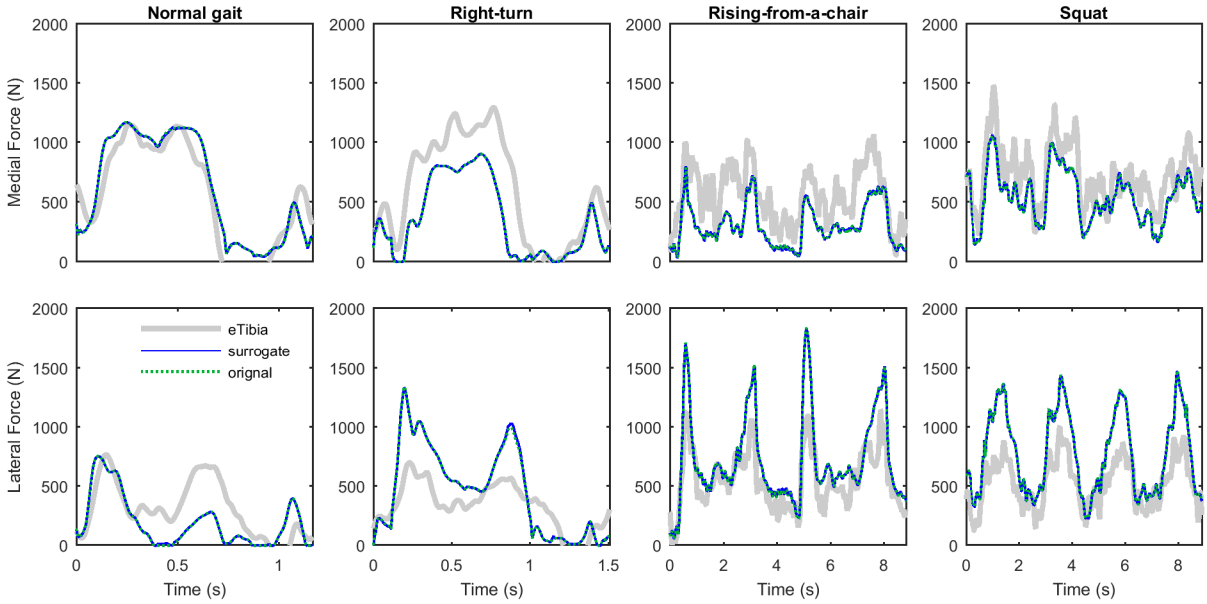
Normal gait
Right-turn
Rising-from-a-chair
Squat
Medial Force (N)
Lateral Force (N)
eTibia
surrogate
orignal
Time (s)

712

714 **Figure 4**

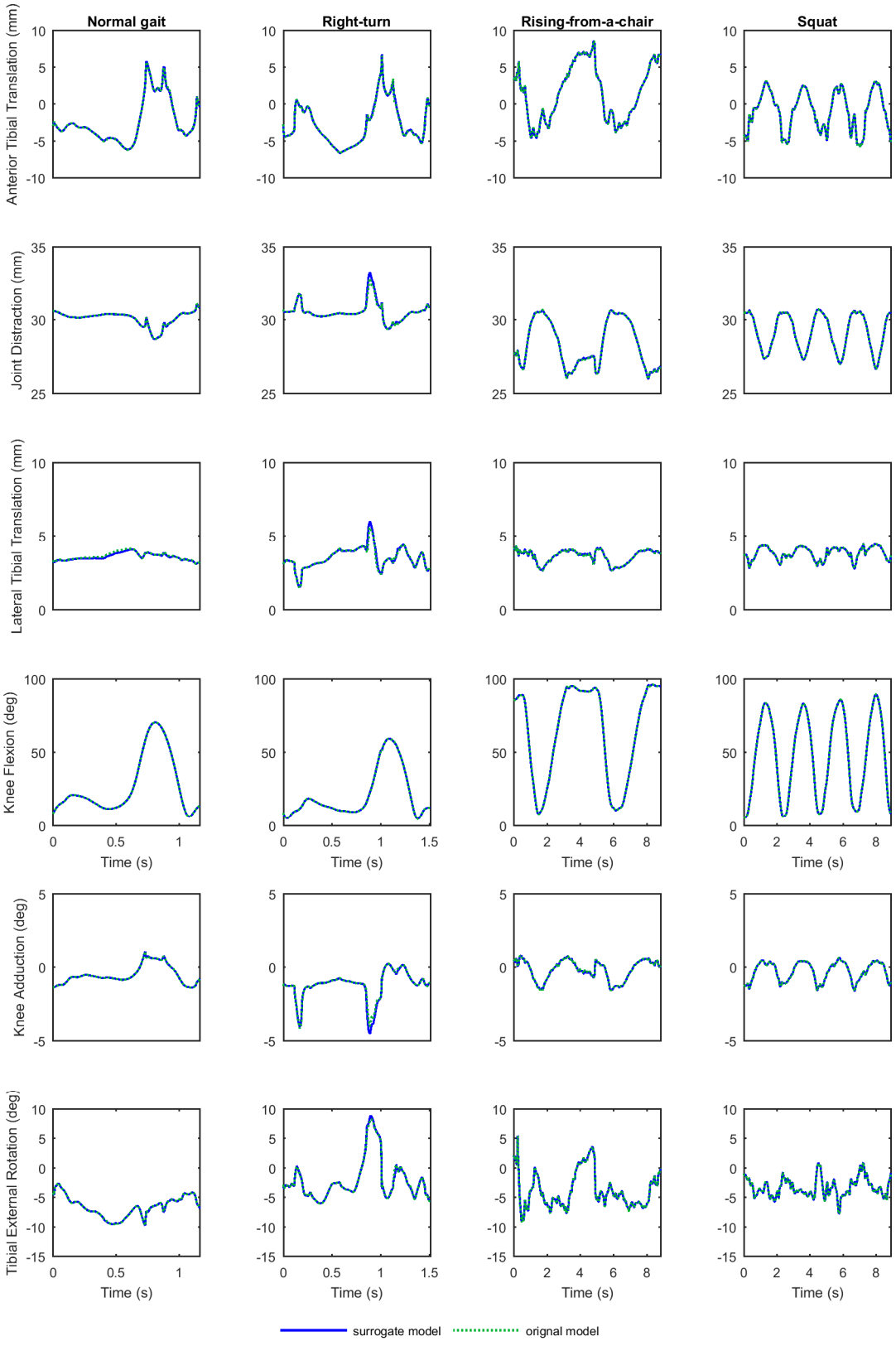
Normal gait
Right-turn
Rising-from-a-chair
Squat
Anterior Tibial Translation (mm)
Joint Distraction (mm)
Lateral Tibial Translation (mm)
Knee Flexion (deg)
Knee Adduction (deg)
Tibial External Rotation (deg)
Time (s)
surrogate model
orignal model